Indian Journal of Biochemistry & Biophysics
Vol. 63, May 2026, pp. 596-605
DOI: 10.56042/ijbb.v63i5.27839

Photodynamic activity of meso-substituted cationic pyridyl porphyrin Zn-TOEt4PyP and its non-covalent interaction product with folic acid

Lusine Mkrtchyan[1], Nikolay Avtandilyan[2], Anzhela Galstyan[3], Anna Zakoyan[1], Edita Nadiryan[2], Rafayel Muradyan[4], Grigor Gyulkhandanyan[1]*, Lusine Danielyan[5] & Torgom Seferyan[3]

[1]Laboratory of Bioengineering, Institute of Biochemistry after H. Buniatyan, NAS RA, 5/1 Paruyr Sevak street, Yerevan 0014, Armenia

[2]Laboratory of Basic and Pathological Biochemistry, Research Institute of Biology, Department of Biochemistry, Microbiology and Biotechnology, Yerevan State University, Yerevan 0025, Armenia

[3]Laboratory of Biomedical research, Institute of Biochemistry after H. Buniatyan, NAS RA, 5/1 Paruyr Sevak street, Yerevan 0014, Armenia

[4]Laboratory of Chemotherapy and Toxicology, Institute of Fine Organic Chemistry after A. L. Mnjoyan of Scientific Technological Center of Organic and Pharmaceutical Chemistry of NAS RA, Yerevan 0014, Armenia

[5]Department of Clinical Pharmacology, University Hospital of Tübingen, Auf der Morgenstelle 8, D-72076, Tübingen, Germany

Received 22 January 2026; *revised 19 March 2026*

This study aims to investigate the efficacy of zinc meso-tetra [4-N- (2'-oxyethyl) pyridyl] porphyrin (Zn-TOEt4PyP) and its non-covalent interaction product with folic acid (FA) for targeted Photodynamic therapy (PDT), taking into account the significant overexpression of FA receptors on tumor cells. Liposomal models were employed to demonstrate lipid free radical chain peroxidation induced by photosensitizer (PS) activation, with FA enhancing this effect. PDT effect of PS and its non-covalent interaction product (NCIP) with FA on HeLa cells culture model were analyzed (*in vitro)* at a maximum density of 3×10^5 cells/well under light exposure. The assessment of the antitumor activity of Zn-TOEt4PyP metalloporphyrin and its NCIP with FA was carried out *in vivo* on the engrafted solid tumor model of S-180 sarcoma (Croker's sarcoma). Zn-TOEt4PyP, its NCIP with FA, and FA itself led to the successful free radical oxidation of liposomes that were utilized as a model of the lipid bilayer. The interaction product of Zn-TOEt4PyP with FA was active as a cytotoxic agent for HeLa cells. The *in vivo* study demonstrated the superior efficacy of Zn-TOEt4PyP over its NCIP with FA in tumor reduction. These findings show efficiency of Zn-TOEt4PyP and its NCIP's with FA for targeted PDT of tumors. Through liposomal, cellular, and animal models, this research provides a comprehensive insight into the efficiency of Zn-TOEt4PyP and NCIP with FA for PDT of tumors *in vitro* and *in vivo*. This study holds significant promise for developing novel PDT strategies to improve cancer treatment outcomes.

Keywords: Metalloporphyrin, Photosensitizers, Reactive oxygen species, Targeted photodynamic therapy

Photodynamic therapy (PDT) is a therapeutic approach that generates reactive oxygen species (ROS), such as singlet oxygen, in the illuminated area of tumors or microbes[1]. It relies on a photosensitizer (PS), light, and molecular oxygen to produce a photodynamic response[2]. When exposed to visible light, the PS transitions to an excited triplet state (3PS), leading to ROS formation (*e.g.*, $^1O_2$, ·OH) that selectively kills cancer cells[3]. Since cancer cells maintain a delicate balance between ROS and antioxidants, PDT disrupts this equilibrium, triggering oxidative stress and releasing free radicals[4]. Highly reactive oxygen species (ROS) generated during PDT lead to the death of cancer cells through two types of reactions: Type I reactions, which produce superoxide anion radicals, hydrogen peroxide, and hydroxyl radicals, and Type II reactions, which generate singlet oxygen ($^1O_2$)[5]. Both reactions can occur simultaneously during PDT; however, Type II is the dominant pathway[6]. The oxidative stress caused by ROS primarily affects macromolecules, such as lipids, proteins, and nucleic acids[7]. ROS interacts with lipids and proteins in cell membranes, causing lipid chain peroxidation and facilitating the spread of free radicals, which further damage cellular integrity[8]. Cell membrane lipids are particularly susceptible to oxidative attack, which makes liposomal systems ideal to study lipid peroxidation, and oxidative effects in the absence of antioxidant defences, as well as to determine the compound with the most powerful effect. Testing biological membrane models for lipid peroxidation is typically conducted by

*Correspondence:
E-mail: grigor.gyulkhandanyan@biochem.sci.am
Suppl. data available on respective page of NOPR

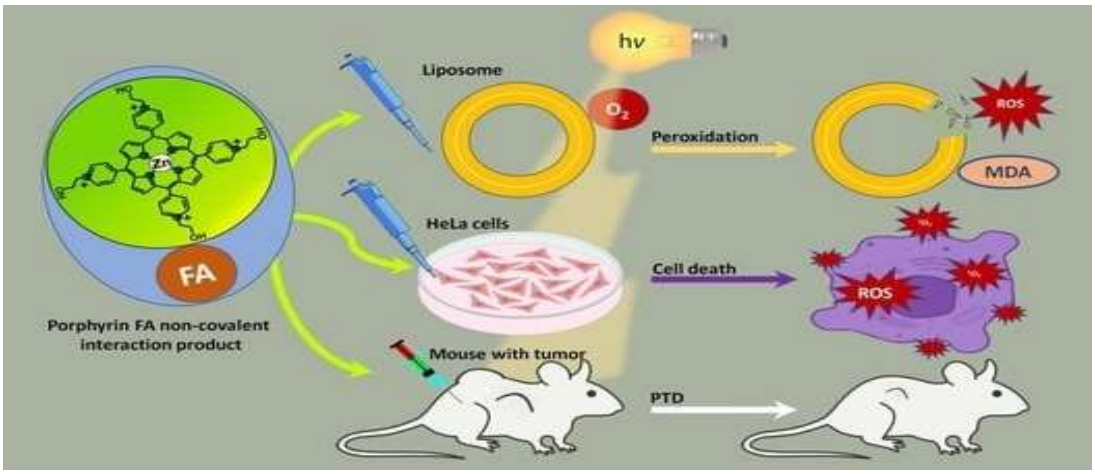

Graphical abstract

analyzing secondary oxidation products, such as malondialdehyde (MDA). Generally, thiobarbituric acid (TBA) test has been used for the detection of MDA for *in vitro* and *in vivo* conditions[9]. Liposome models help investigate the direct effects of PS and their non-covalent interactions with FA on membrane lipid bilayers. Liposomes composed solely of lipids can serve as models to investigate the effect of PS on membrane lipids (primarily phospholipids) by monitoring MDA production levels following PS activation by light[10].

In our study, cationic porphyrin Zn-TOEt4PyP was used as PS to examine the photoactivated disruption of membrane physiology.

Targeted drug delivery to tumor sites remains a critical challenge, and leveraging cancer cell properties is a key strategy for effective PDT. Since FA receptors are overexpressed in human cancer cells—at levels 100–300 times higher than in normal tissues—FA serves as a valuable targeting agent, enabling precise drug delivery[11]. Folate receptors are overexpressed on prostate, brain, lung, nose, ovary, colon, cancer cells and have very low expression on normal cells. This selective overexpression makes folate receptors attractive targets for tumor-specific delivery when folic acid (FA) is conjugated to anticancer molecules. HeLa cells are well known to express folate receptors on their surface and are commonly used as a folate receptors-positive model to evaluate folate-targeted uptake and photodynamic therapy efficacy[12,13]. To enhance PDT efficacy, we utilized NCIPs of PS with FA.

In the presented manuscript we investigated the ability of Zn-TOEt4PyP and its NCIP with FA to oxidize lipids in the liposomal model following photodynamic action, as well as the anticancer potential of Zn-TOEt4PyP and its NCIP with FA through both *in vitro* (HeLa cells) and *in vivo* (S-180 sarcoma mouse model) studies.

Materials and Methods

Porphyrins

The cationic metalloporphyrin (zinc meso-tetra [4-N- (2'-oxyethyl) pyridyl] porphyrin) synthesized in Yerevan State Medical University after M. Heratsi, (RA) in collaboration with ARLABION Co. Ltd (UK) with chemical structure depicted in (Fig. 1). FA was obtained from the ACROS Organics (Folic Acid, 97% pure; Product code 216630100, CAS Number: 59-30-3). The NMR spectrum, as well as the MS spectrum of Zn-TOEt4PyP metallo-porphyrin is provided in the supplementary information of the manuscript (Suppl. Figs. S1 & S2). The zinc(II) metallocomplex of the 5,10,15,20-tetra[4-N-(2/oxyethylpyridyl)]porphinetetrachloride, ZnTOEt4PyP, was prepared by refluxing the mixture of zinc(II) chloride ($ZnCl_2$) and H2TOEt4PyP similarly, to that described in this article in the same way that as for the complexes 5,10,15,20-tetra(4-N-allylpyridyl) porphinato Zn(II) tetrabromide, ZnTAll4PyP (Suppl. Figs. S1 & S2)[14,15].

Non-covalent interaction of FA and PS

As it was previously described, the interaction products were obtained using the method developed in our laboratory[16]. In brief, FA and PS were incubated at +20°C for 24 h in the dark, with a 5-fold excess in FA. Glycerol, with a final concentration of 20% was added to the reaction mixture, which was then incubated for a further 24 h. Glycerol was employed as a stabilizer for FA. As glycerol is an optical clearing agent that increases the depth of light

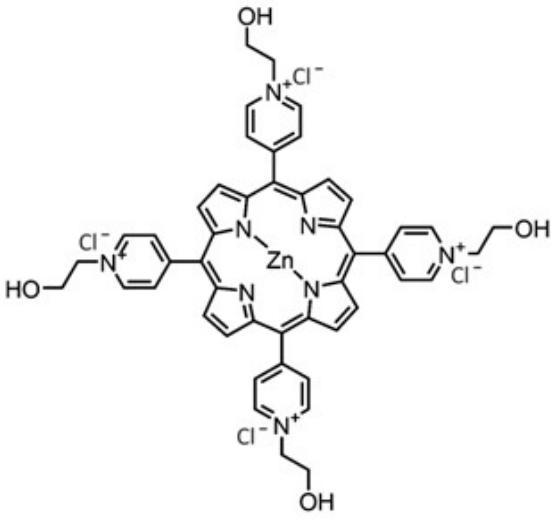

Fig. 1 — Chemical structure of cationic metalloporphyrin Zn-TOEt4PyP

beam penetration into tumor tissue, it is predicted to have a synergistic impact when used with PDT during both stages of treatment: preliminary fluorescence mapping of cancer cells and photodestruction[17-20]. The unbound components were purified, by Al_2O_3 (aluminium oxide) column chromatography. 0.1 M phosphate-buffered saline (PBS) containing 20% glycerol was used as eluent. The absorption spectra of the fractions across a wavelength range of 200-700 nm where obtained by Cary 60 UV-Vis Spectrophotometer (Agilent Co., USA). The FA/PS concentration ratio in NCIP was 6.3/1.PS and FA concentrations were determined using UV-Vis spectrum extinction coefficients[21].

Liposome model

Egg yolk total lipids were isolated by the Folch method[22] from fresh eggs of Broiler chickens farmed in the vivarium of Institute of Biochemistry after H. Buniatyan of the NAS of RA. For the preparation of the liposome suspension, 0.77 mL of chloroform-methanol solution containing egg yolk total phospholipids at a concentration of 2.1 g/L was evaporated using a rotary evaporator under vacuum and a stream of nitrogen gas, followed by addition of 25 mL saline. Before use, the saline was degassed by bubbling nitrogen through it. The dried lipids were incubated with saline for 40 min in +37°C environment, and then vortexed to create a suspension. The formed suspension was treated by ultrasonic generator UZDN-2T(22 kHz, 200w) for 6 min. Subsequently, the final liposomal suspension was thermally stabilised for 30 min.

MDA level determination

After obtaining the liposome suspension, the tested compound (either FA or Zn-TOEt4PyP, or their NCIP) was added to the liposome suspension and illuminated with a halogen lamp as described previously[16]. The illumination covered a wavelength range of 380 – 850 nm at an irradiance of 30 mW/cm^2. The UV–Vis spectra of FA, Zn-TOEt4PyP, and their NCIP are presented in (Suppl. Figs. S3-S5), respectively. The concentration of the free Zn-TOEt4PyP and Zn-TOEt4PyP in the NCIP was 0.8 μM. The effect of FA was assessed at a final concentration of 6.4 μM in liposome suspension. The FA/PS ratio in the NCIP was set to 8/1. To evaluate the effect of illumination duration on the level of MDA, each sample was illuminated to one of two illumination durations: 5 or 10 min using a halogen lamp with an intensity of 30 mW/cm^2. The concentration of MDA was measured spectrophotometrically on spectrophotometer Cary 60 UV-Vis (Agilent Technologies, Inc., USA) at 532 nm using the TBA test[23]. The formed MDA-TBA complexes were extracted and quantified with the addition of 2 mL of n-butanol to each sample.

Quantitative changes of MDA were observed by comparing each illuminated sample with its unilluminated control and expressed as a percentage using the formula (b-a)/(a/100) where a- is the control group (intact liposomes), and b- illuminated samples (liposome+PS, liposome+(PS+FA) or liposome+FA).

Cell culture

HeLa (human cervical carcinoma) cells were maintained in Dulbecco's Modified Essential Medium (DMEM) (Sigma-Aldrich, Taufkirchen, Germany) supplemented with 10% (*v/v*) bovine serum, low glucose (1 g/L), sodium pyruvate (200 mg/L), and antibiotics (100 U/mL penicillin and 100 μg/L streptomycin). The cells were cultured in 96-well microplates at a maximum density of 3×10^5 cells/well in an incubator (Biosan S-Bt Smart Biotherm, Latvia) at +37°C with humidified atmosphere containing 5% CO_2.

MTT cytotoxicity assay

The MTT assay (#MKCR0748, Sigma-Aldrich, Taufkirchen, Germany) was conducted to evaluate the inhibitory effect of various concentrations of the Zn-TOEt4PyP photosensitizer on the growth of HeLa cells, both alone and in combination with FA. The concentration of FA in the NCIP for *in vitro* studies was at an 8:1 (*w/w*) ratio with PS. Taking into account

the above mentioned, a 57.6 nM concentration was used to assess the properties of FA on a standalone basis. This corresponds to its concentration in the NCIP, where the combined concentration of Zn-TOEt4PyP and FA is 7.2 nM.

The cells were maintained under dark conditions in a CO_2 incubator for 24h after the addition of compounds. One hour after the addition of compounds, cells were exposed to light for 15 min with halogen lamp (30 mW/cm^2) and kept additional 24h in a CO_2 incubator. The absorbance of the samples at 570 nm was measured by absorbance microplate reader (SPECTROstar Nano BMG Labtech, USA). Four independent experiments were performed with four technical replicates each.

Cytotoxicity was quantified as the percentage of growth inhibition in cells treated with selected compounds compared to control cells treated with the appropriate volume of solvent (0.1M PBS containing 20% glycerol (w/v)), the growth of which was considered as 100%.

Half-maximal inhibitory concentration (IC_{50}) values were calculated by GraphPad Prism Software during data analysis as log (inhibitor) vs. response.

Determination of Zn-TOEt4PyP and its NCIP with FA activity *in vivo*

The assessment of the antitumor activity of Zn-TOEt4PyP metalloporphyrin and its NCIP with FA was carried out *in vivo* on the ingrafted solid tumor model of S-180 sarcoma (Croker's sarcoma). For each experimental group, 9 male non-linearoutbred white albinomice(more than 20 generations of brother/sister mating) aged 6-7 weeks and weighing between 20 to 25 g, were injected with a solid S-180 sarcoma tumor subcutaneouslyinto the right axilla. Tumor tissues removed from sarcoma-180 carrying animal in 8-th day were implanted to experimental animals. Injected tumor suspension was prepared by cutting 1 g solid tumor into pieces (<1 mm^3) in 9 mL saline in sterile conditions. Injections were done by thick needle of 0.3 mL/animal dosage (~10^6 cell/mL)[24]. The animals' fur was pre-depilated. Free PS and the NCIP was administered into the implanted tumor site in a dose of 60 mg/kg in 48 h, 72 h and 96 h after tumor engraftment (20 mg/kg per injection in 0.25 mL volume). The control group of animals were injected with saline into the implanted tumor site. To assess the photodynamic (light) toxicity of Zn-TOEt4PyP and its NCIP with FA, the tumor was irradiated with a halogenlamp (30 mW/cm^2) for 15 min, 24h after the final dose of the compoundswas administrated. Animals were humanely euthanized upon exposure of CO_2 dispatched 8 days (192h) after tumor engraftment and the wet weight of excised tumor was measured and compared with control sample. Antitumor activity was defined as tumor growth inhibition (TGI) by Eq. 2:

$$[\text{TGI, \%}]=[(\text{MTW}_{\text{control}} - \text{MTW}_{\text{experimental group}})/\text{MTW}_{\text{control}}] \times 100\%. \text{(Eq. 2)}$$

Where: (MTW) is median tumor weight.

Animals were housed under controlled conditions (12h light/dark cycle; humidity 60±5%; room temperature +25±3°C).

Ethical review

Biological experiments were performed in full compliance with the ethical principles of biomedical research reflected in the European Convention for the Protection of Vertebrate Animals used for Experimental and Other Scientific Purposes and approved by the Committee on Biomedical Ethics at the Institute of Biochemistry named after H. Buniatyan of the NAS RA. The experiments also comply with the Directive 2010/63/EU of the European Parliament and of the Council of the European Union of 22.09.2010 on the protection of animals used for scientific purposes, Strasbourg, No. 123, 18.03.1986[25,26].

Statistical analysis

The result was reported as mean ± standard error of the mean (SEM). Data were analysed using one-way ANOVA or Student's *t*-test with GraphPad Prism Software (GraphPad Software Inc, La Jolla, CA, USA). Statistical significance is indicated as follows: ns (not significant): $P > 0.05$, *: $P \leq 0.05$, **: $P \leq 0.01$, ***: $P \leq 0.001$, ****: $P \leq 0.0001$ (Graph Pad 8).

Results

MDA level measurements

After adding the compounds (FA, Zn-TOEt4PyP, and non-covalent NCIP (FA+Zn-TOEt4PyP)) to the liposome suspension, the MDA level was determined by the TBA test in both the dark control and the test samples, which were illuminated for 5 and 10 min respectively. The addition of FA to liposome suspension led to the lipid peroxidation and to the production of the secondary product MDA (Fig. 2).

The increase in illumination duration led to more intense MDA production in all samples proving that

the lipid peroxidation was induced by the free radical generated by PS molecule under light exposure (Fig. 2). Of note, a significant increase was observed after 5 min of illumination, while a non-significant increase was recorded after 10 min of illumination in the tested groups.

The cytotoxic effect of Zn-TOEt4PyP and Zn-TOEt4PyP+FA NCIP on the HeLa cell line

We compared the cytotoxic effects of the photosensitizer Zn-TOEt4PyP, the Zn-TOEt4PyP+FA NCIP, and FA on the HeLa cervical cancer cell line by assessment of cell survival rate under both light and dark conditions. The effects of both the Zn-TOEt4PyP alone and its combination with FA NCIP were evaluated at different concentrations, as shown in (Fig. 3). The obtained data demonstrate significant decrease in cell viability when Zn-TOEt4PyP and TOEt4PyP+FA was exposed to light for 15 min. Specifically, for Zn-TOEt4PyP, a notable significant cytotoxic effect began at a concentration of 7.2 nM (38% inhibition), and the highest significant effect of inhibiting the growth of HeLa cells was observed at 36 nM (67% inhibition) (Fig. 3a). For the Zn-TOEt4PyP+FA NCIP, significant cytotoxic effects were noted starting at 0.72 nM (17% inhibition), and the highest significant effect (73% inhibition) was observed at 36 nM (Fig. 3b). This indicates that the light exposure contributed to the decrease in cell viability.

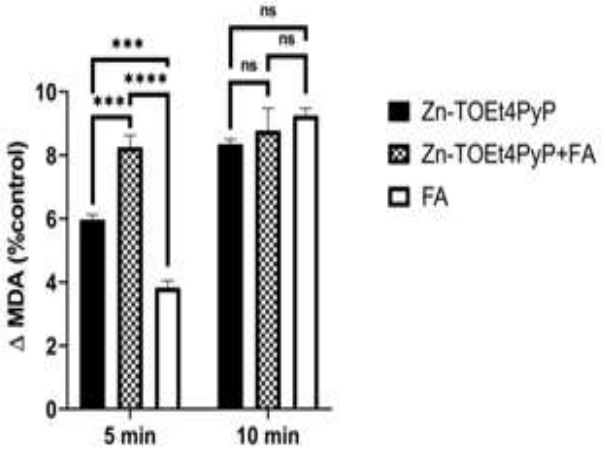

Fig. 2 — The percentage of difference (Δ) of MDA following the illumination of the samples with Zn-TOEt4PyP, Zn-TOEt4PyP+FA, and FA, (difference calculated by comparison with control and unilluminated liposomal suspensions were employed as controls (100%)). The data are presented as means ± SEM (n=5). Differences between groups were analysed using one-way ANOVA. Statistical significance is indicated as follows: (ns) $P > 0.05$, (***) $P \leq 0.001$, (****) $P \leq 0.0001$

Separately the growth inhibitory properties of FA alone on the HeLa cervical cancer cell line were explored with and without light treatment at 57.6 nM concentration (Fig. 3c). A slight inhibitory effect was detected under both light and dark conditions, without reaching the statistical significance. Thus, based on

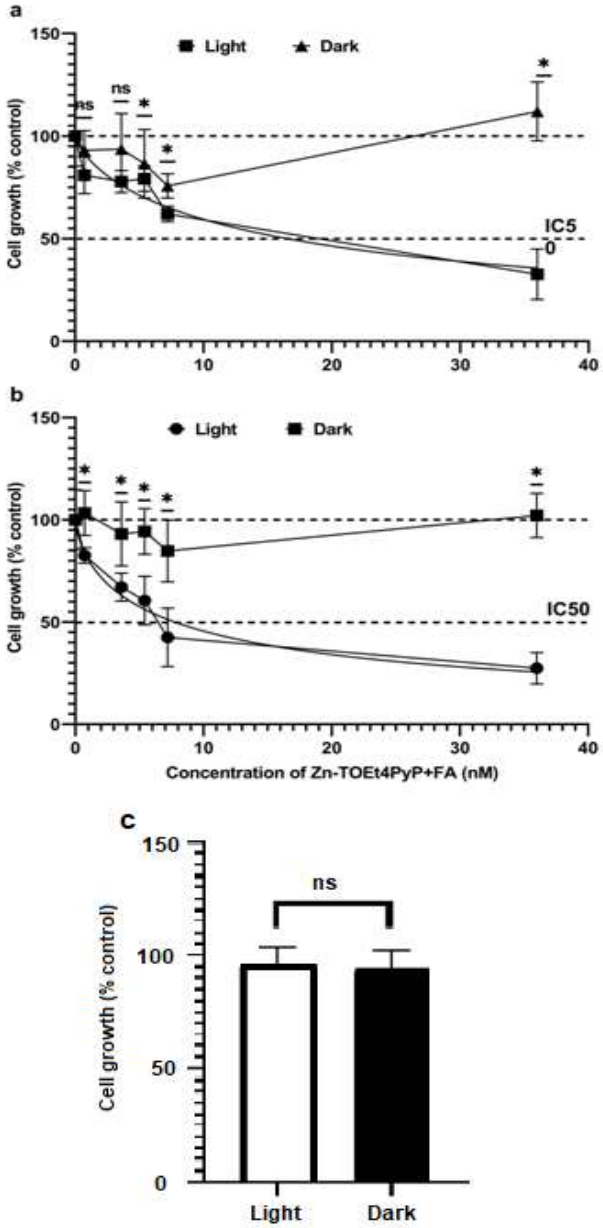

Fig. 3 — Growth inhibitory effect of the (a) photosensitizer Zn-TOEt4PyP; (b) Z-TOEt4PyP + FA NCIP; and (c) FA on the HeLa cervical cancer cell line with and without light treatment. Cells were maintained in a CO_2 incubator for 24h after exposure to light for 15 min with a halogen lamp (30 mW/cm^2). The data are presented as means ± SEM (n=5). Differences between groups were analysed using multiple t-test and One-way ANOVA. Statistical significance is indicated as follows: (ns) $P > 0.05$, (*) $P \leq 0.05$

Table 1 — The key photophysical and biological properties of FA, Zn-TOEt4PyP, and Zn-TOEt4PyP+FA NCIP

	absorption maxima (nm)	molar extinction coefficient (ε), ($M^{-1}\cdot cm^{-1}$)	quantum yield of singlet oxygen (γΔ)	emission maxima (nm)	IC_{50} (nM)
FA	280 and 350	0.02522 x 10^6	≤ 0.02[31]	excitation 370, emission 450	>35
Zn-TOEt4PyP	439	$1.433 \cdot 10^5$	0.84±0.04	excitation 440, emission 637	7.737
Zn-TOEt4PyP+FA NCIP	446 for Zn-TOEt4PyP and 283 for FA	Same, no changes	0.83±0.04	same for components	16.52

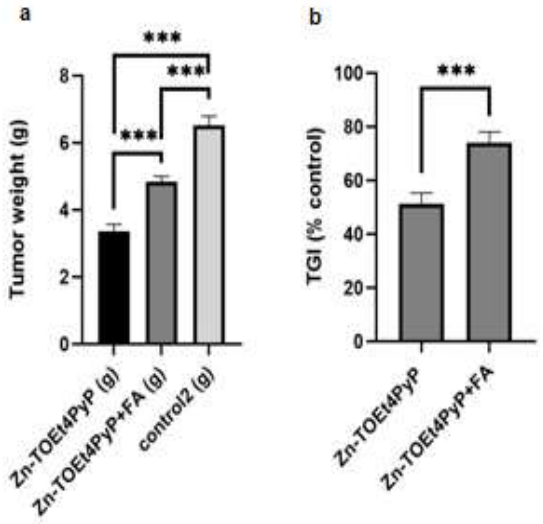

Fig. 4 — The effect of PDT on Sarcoma S-180 tumor weight (g) 192h (8 days) after tumor engraftment. Administration of saline (to control group), the free PS ((Zn-TOEt4PyP) and the NCIP (Zn-TOEt4PyP+FA) were done in a dose of 60 mg/kg in 48 h, 72 h and 96 h after tumor engraftment. Each tumor was irradiated with a halogen lamp (30 mW/cm^2) for 15 min, 24h after the final dose of the drug was administered. After resection, tumors weights were measured (a) and compared with the control sample; and (b) Antitumor activity after PDT, which was defined as tumor growth inhibition (TGI %) by Eq. 2. indicated in the methods section. The data are presented as means ± SEM (n=9). Differences between groups were analysed using one-way ANOVA. Statistical significance is indicated as follows: (***) $P \leq 0.001$

the obtained data we showed that Zn-TOEt4Pyp did not possess cytotoxicity itself and needs exposure of light to become a potent toxic agent for the HeLa cancer cell line. We also demonstrated that the presence of FA did not have a significant effect on the cytotoxicity of the tested photosensitizer. A slight increase in cytotoxicity was observed, which could be explained by the synergistic action of FA and Zn-TOEt4PyP, or as expected, by receptor-mediated endocytosis facilitated by the FA receptor and slightly increased accumulation of the photosensitizer (PS) (Fig. 3c). Half-maximal inhibitory concentration (IC_{50}) values were calculated to compare the effect of FA on the growth-inhibiting properties of the tested compound (free PS vs NCIP). Calculations revealed that binding of FA to PS significantly affected these values, being 16.52 for Zn-TOEt4PyP and 7.737 for Zn-TOEt4PyP+FA.

The cytotoxic activity assessment of Zn-TOEt4PyP and its NCIP with FA *in vivo*

We also assessed the cytotoxic effects of Zn-TOEt4PyP and its NCIP with FA using a Sarcoma S-180 mouse model *in vivo*, administering a dose of 60 mg/kg body weight for both the free PS and NCIP (Suppl. Fig. S6).

As shown in Figure 4, Zn-TOEt4PyP was by 1.88 times more effective than its NCIPZn-TOEt4PyP+FA in reducing the tumor weight.

The key photophysical and biological properties of FA, Zn-TOEt4PyP, and Zn-TOEt4PyP+FA NCIP are presented in (Table 1).

Limitations of the study

Although the present study demonstrates the photodynamic cytotoxicity and antitumor activity of Zn-TOEt4PyP and its non-covalent interaction product with folic acid, some mechanistic aspects of their biological activity remain to be further elucidated. In particular, the molecular mechanisms underlying the differences observed between the two formulations *in vivo* were not investigated in detail. Future studies may focus on deeper mechanistic analysis, including cellular uptake pathways, intracellular localization, and reactive oxygen species–mediated signaling processes involved in photodynamic cell death. In addition, further evaluation in tumor models derived from specific cell lines (including the HeLa cells xenograft model) could provide additional insight into the relationship between cellular phototoxicity and antitumor efficacy.

Discussion

Encapsulation and bioconjugation of PSs are currently the main strategies for improving PDT[27]. To

date various nanosystems have been developed for encapsulation and binding anticancer molecules to increase their tumor delivery and therapeutic efficacy[28]. In order to achieve greater PS efficiency, a simpler approach of non-covalent interaction of cationic metalloporphyrin Zn-TOEt4PyP with FA has been applied in the current study. Our data reveals the characterization of a PS Zn-TOEt4Py and its NCIP with FA. Here we applied different *in vitro* models (liposome and cell experiments) and an *in vivo* tumor model to explore the free radical oxidative photodynamic action of both the free PS and the PS in combination with FA. For FA, a linear increase in MDA generation has been observed with increasing durations of the illumination. FA is known for its antioxidant, cardiovascular, anticancer, and neuroprotective effects[29]. In the present study, the illumination of FA led to a related MDA generation effect as opposed to the antioxidant effect. This can be explained by the FA photolysis into p-aminobenzoyl-L-glutamic acid (PGA) and 6-formylpterin (FPT), which is then further oxidized to pterin-6-carboxylic acid (PCA) by photolysis. FPT and PCA, in their turn, can act as PS[21], and generate ROS, which induces lipid oxidation and increases MDA concentration[30]. FA itself behaves as a poor $^1O_2$ sensitizer due to its low singlet quantum yield ($\leq$0.02)[31]. For FPT, the value of singlet quantum yield was 0.45 ± 0.05 and for PCA it was 0.27 ± 0.03, which allows to conclude that this product could act as PS[31].

The increase in illumination duration from 5 to 10 min, led to the increase in MDA level in liposome models, up to 9.2%, likely caused by the photoproducts of FA photolysis. Therefore, we concluded that MDA production is initiated by photoactive FPT and PCA as products of FA photolysis.

It is worth mentioning that, the MDA assay has limitations due to its potential reactivity with various compounds which can interfere with spectrophotometric and fluorometric measurements of MDA[32]. The accessibility of MDA to TBA may be reduced due to multiple reactions of TBA with chemically reactive carbonyl-containing organic molecules, such as reduced sugar, aldehydes, pyrimidines, aminopyrimidines, and prostaglandin endoperoxides[33,34]. Other limitations include low MDA stability in samples and its rapid enzymatic degradation[35]. MDA's instability in the presence of H_2O_2 suggests its direct decomposition by strong oxidants. In addition, TBA reagent may chemically degrade during the acid-heating test procedure to yield pigments[36].

Therefore, as noted, the lack of sensitivity and the occurrence of byproducts create obstacles a problem for detection of lipid peroxidation levels through a TBA test.

In addition, it cannot be excluded that in the sample of liposomes with PS, the competing reaction of MDA to TBA binding could also occur, and as a result, the accessibility for forming the MDA-TBA could be limited. We have assumed that the ROS production, following the illumination, could lead to changes in the formation or even to the destruction of the formed MDA-TBA colored complex. Therefore, due to the increase in illumination duration, a non-linear dependency could be observed.

It was previously demonstrated that the singlet oxygen quantum yield of Zn-TOEt4PyP is as high as 0.85[37]. Thus, Zn-TOEt4PyP as an effective $^1O_2$ producer could lead to intense peroxidation of liposomes and further reactions. As shown in Figure 2, the generation of MDA for FA and Zn-TOEt4PyP following a 10 min illumination is almost the same, although the singlet oxygen quantum yield of Zn-TOEt4PyP's is 1.89-fold higher than that of the FA photolysis product FPT. This could mean that singlet oxygen generation is not the only factor affecting lipid peroxidation. As in our previous study, the use of quenchers demonstrated the role of both singlet oxygen and hydroxyl radicals in oxidation reactions[16]. All this leads to the conclusion that attests to the NCIP-ity of the studied system. In the studied NCIP, the singlet oxygen quantum yield of Zn-TOEt4PyP was not affected by FA[16], and the results obtained for the TBA assay were similar.

It should also be noted that PSs lead to an increase of MDA level after illumination. This effect was demonstrated for many PSs such as aminolevulinic acid[38], Photofrin II[39], tin(IV)-protoporphyrin IX[40], berberine[41], TCSVP[42], *etc*.

For the HeLa cell line, no statistically significant cell growth inhibiting properties were observed under dark conditions, which allow concluding that light exposure is necessary for Zn-TOEt4PyP to become cytotoxic and act as a PS. Moreover, light growth stimulation was detected at high concentrations of Zn-TOEt4PyP and the Zn-TOEt4PyP+FA NCIP. Zn-TOEt4PyP+FA NCIP showed a more significant inhibitory effect under these conditions. As it is shown, from IC_{50} values NCIP have 53% more inhibitory effectivity.

Porphyrins, particularly Zn-porphyrins, exhibit high cell toxicity due to their strong p-p interactions, having a potential for tumor destruction[2].

HeLa cells highly express FA receptors[43]; and are among the most widely used cell lines for FA-PS conjugation studies. In most cases, coupling the PS with FA leads to enhanced similar cell growth inhibitory cytotoxicity effects[13]. Thus, this cell line was used as the *in vitro* model to study the targeting of Zn-TOEt4PyP. As reported in 2013 study by Li et al, the photocytotoxicity of a folate–PEG-conjugated chlorine to HeLa cells is 2.5 higher than folate-free conjugate chlorine. Significant difference by utilizing FA as the targeting agent for IC_{50} where observed as well. In another study (by Bae and Na,[44]), both the Pullulan/folate-PS nanogels, and free pheophorbide APullulan/folate-PS also showed almost the same significant cytotoxicity (IC_{50}; PFP2: 0.23 mg/mL; Pullulan/folate-PS: 0.2 mg/mL) following illumination.

For the Sarcoma S-180 tumor model, we did not obtain results similar to those observed in the HeLa cell line model. Both Zn-TOEt4PyP and Zn-TOEt4PyP+FA NCIP exhibited significant PDT-induced TGI compared to the control group. However, in contrast to the HeLa cell line model, Zn-TOEt4PyP+FA NCIP demonstrated lower PDT activity compared to Zn-TOEt4PyP alone. This difference may be attributed to variations in cancer cell and tumor type, as well as systemic differences between *in vitro* and *in vivo* conditions. Additionally, the potential binding of Zn-TOEt4PyP+FA to plasma proteins such as albumin, may have influenced its bioavailability and distribution[45]. Other contributing factors could include hemodynamics and tissue structure.

The use of complementary experimental systems (model membrane systems, cultured tumor cells, and an *in vivo* tumor model) allows assessment of both direct cellular phototoxicity and the overall antitumor effect in a living organism. The differences observed between the activities of Zn-TOEt4PyP and Zn-TOEt4PyP+FA NCIP in the S-180 tumor model may be influenced by several biological factors present *in vivo*, including tumor microenvironment, biodistribution of the photosensitizer, and the stability or interaction dynamics of the non-covalent complex.

The obtained results are likely explained by the non-covalent binding of the PS with FA, leading to less effective targeting of cancer cells *in vitro*.

Conclusion

The tested photosensitizer and its non-covalent interaction product with folic acid enhance the oxidation of membrane lipids, leading to the production of malondialdehyde, a secondary product of lipid peroxidation in the liposomal model. This suggests their potential application in photodynamic therapy for tumors. The non-covalent interaction product of the studied photosensitizers exhibits a greater inhibitory effect on the HeLa cell growth compared to the free form of the photosensitizer. Due to various factors, including the binding of plasma proteins with folic acid, the non-covalent interaction product of the tested photosensitizer with folic acid did not exhibit a greater inhibitory effect on the *in vivo* Sarcoma S-180 tumor model compared to the free form of the photosensitizer. Despite the studied potential of metalloporphyrins for photodynamic therapy and the concept of utilizing folic acid receptor overexpression in cancer cells as a key strategy for targeted therapy, the experimental results presented in this paper vary between *in vitro* and *in vivo* models.

Acknowledgement

Authors express their gratitude to Prof. Gilles Gasser as well as to Dr. João P. M. António from Chimie ParisTech, PSL University, CNRS Institute of Chemistry for Life and Health Sciences, Laboratory for Inorganic Chemical Biology, for the NMR and MS spectra of compounds, obtained in Paris, France. This work was supported by the Ministry of Education, Science, Culture and Sport of the Republic of Armenia Higher Education and Science Committee and Belarusian Republican Foundation for Fundamental Research in the frames of the joint research project HESC No 21SC-BRFFR-1F007 and BRFFR grant № Ф21ARM-014 respectively.

This project was also supported by the Federation of the European Biochemical Societies Collaborative Developmental Scholarship, 2022.

Conflict of interest

All authors declare no conflict of interest.

References

1 Shui S, Zhao Z, Wang H, Conrad M & Liu G, Non-enzymatic lipid peroxidation initiated by photodynamic therapy drives a distinct ferroptosis-like cell death pathway. *Redox Biol*, 45 (2021) 102056.

2 Rong Y, Hong G, Zhu N, Liu Y, Jiang Y & Liu T, Photodynamic Therapy of Novel Photosensitizer Ameliorates TNBS-Induced Ulcerative Colitis *via* Inhibition of AOC1. *Front Pharmacol*, 12 (2021) 746725.

3 Smith CB, Days LC, Alajroush DR, Faye K, Khodour Y, Beebe SJ & Holder AA, Photodynamic Therapy of Inorganic Complexes for the Treatment of Cancer†. *Photochem Photobiol*, 98 (2022) 17.

4 Cho G, Lee D, Kim SM & Jeon TJ, Elucidation of the Interactions of Reactive Oxygen Species and Antioxidants in Model Membranes Mimicking Cancer Cells and Normal Cells. *Membranes*, 12 (2022) 286.

5 Weishaupt KR, Gomer CJ & Dougherty TJ, Identification of singlet oxygen as the cytotoxic agent in photoinactivation of a murine tumor. *Cancer Res*, 36 (1976) 2326.

6 Ormond A & Freeman H, Dye Sensitizers for Photodynamic Therapy. *Materials*, 6 (2013) 817.

7 Ion RM & Suica-Bunghez IR, Oxidative Stress-Based Photodynamic Therapy with Synthetic Sensitizers and/or Natural Antioxidants In: *Basic Principles and Clinical Significance of Oxidative Stress*. (Ed. by Gowder SJT, InTech), 2015.

8 Saczko J, Photo-oxidative action in MCF-7 cancer cells induced by hydrophobic cyanines loaded in biodegradable microemulsion-templated nanocapsules. *Int J Oncol*, 41 (2012) 105.

9 Kaurinovic B & Popovic M, Liposomes as a Tool to Study Lipid Peroxidation In: *Lipid Peroxidation*. (Ed. by Catala A, InTech), 2012.

10 Bacellar IOL & Baptista MS, Mechanisms of Photosensitized Lipid Oxidation and Membrane Permeabilization. *ACS Omega*, 4 (2019) 21636.

11 Parveen S & Sahoo SK, Evaluation of cytotoxicity and mechanism of apoptosis of doxorubicin using folate-decorated chitosan nanoparticles for targeted delivery to retinoblastoma. *Cancer Nano*, 1 (2010) 47.

12 Bellotti E, Cascone MG, Barbani N, Rossin D, Rastaldo R, Giachino C & Cristallini C, Targeting Cancer Cells Overexpressing Folate Receptors with New Terpolymer-Based Nanocapsules: Toward a Novel Targeted DNA Delivery System for Cancer Therapy. *Biomedicines*, 9 (2021) 1275.

13 Stallivieri A, Baros F, Jetpisbayeva G, Myrzakhmetov B & Frochot C, The Interest of Folic Acid in Targeted Photodynamic Therapy. *CMC*, 22 (2015) 3185.

14 Tovmasyan AG, Babayan NS, Sahakyan LA, Shahkhatuni AG, Gasparyan GH, Aroutiounian RM & Ghazaryan RK, Synthesis and *in vitro* anticancer activity of water-soluble cationic pyridylporphyrins and their metallocomplexes. *J Porphyrins Phthalocyanines*, 12 (2008) 1100.

15 Pozza MD, Mesdom P, Abdullrahman A, Prieto Otoya TD, Arnoux P, Frochot C, Niogret G, Saubaméa B, Burckel P, Hall JP, Hollenstein M, Cardin CJ & Gasser G, Increasing the π-Expansive Ligands in Ruthenium(II) Polypyridyl Complexes: Synthesis, Characterization, and Biological Evaluation for Photodynamic Therapy Applications. *Inorg Chem*, 62 (2023) 18510.

16 Mkrtchyan L, Seferyan T, Parkhats M, Lepeshkevich S, Dzhagarov B, Shmavonyan G, Tuchina E, Tuchin V & Gyulkhandanyan G, The role of singlet oxygen and hydroxyl radical in the photobleaching of meso-substituted cationic pyridyl porphyrins in the presence of folic acid. *J Innov Opt Health Sci*, 17 (2024) 2440002.

17 Jaafar A, Darvin ME, Tuchin VV & Veres M, Confocal Raman Micro-Spectroscopy for Discrimination of Glycerol Diffusivity in Ex Vivo Porcine Dura Mater. *Life*, 12 (2022) 1534.

18 Pires L, Demidov V, Wilson BC, Salvio AG, Moriyama L, Bagnato VS, Vitkin IA & Kurachi C, Dual-Agent Photodynamic Therapy with Optical Clearing Eradicates Pigmented Melanoma in Preclinical Tumor Models. *Cancers*, 12 (2020) 1956.

19 Tuchina DK, Meerovich IG, Sindeeva OA, Zherdeva VV, Savitsky AP, Bogdanov AA & Tuchin VV, Magnetic resonance contrast agents in optical clearing: Prospects for multimodal tissue imaging. *J Biophotonics*, 13 (2020) e201960249.

20 Tučin VV, Zhu D & Genina EA, eds., *Handbook of Tissue Optical Clearing: New Prospects in Optical Imaging* (First edition. CRC Press, Taylor & Francis Group) 2022.

21 Off MK, Steindal AE, Porojnicu AC, Juzeniene A, Vorobey A, Johnsson A & Moan J, Ultraviolet photodegradation of folic acid. *J Photochem Photobiol B: Biol*, 80 (2005) 47.

22 Folch J, Lees M & Sloane Stanley GH, A simple method for the isolation and purification of total lipides from animal tissues. *J Biol Chem*, 226 (1957) 497.

23 Draper HH, Squires EJ, Mahmoodi H, Wu J, Agarwal S & Hadley M, A comparative evaluation of thiobarbituric acid methods for the determination of malondialdehyde in biological materials. *Free Radic Biol Med*, 15 (1993) 353.

24 Yeganyan LR, Muradyan RE, Arsenyan FH, Bazikyan GK & Ayrapetyan SN, Magnetically treated water at 4 Hz and 2.5 mT as a modulator of cisplatin effect on cell hydration and ouabain binding of sarcoma-180 tissue. *Environmentalist*, 32 (2012) 236.

25 Directive - 2010/63 - EN - EUR-Lex. Accessed May 8, 2025.

26 Eiropas konvencija par izmēģinājumos un citos zinātniskos nolūkos izmantojamo mugurkaulnieku aizsardzību LIKUMI.LV. Accessed May 8, 2025.

27 Mfouo-Tynga IS, Dias LD, Inada NM & Kurachi C, Features of third generation photosensitizers used in anticancer photodynamic therapy: Review. *Photodiagnosis Photodyn Ther*, 34 (2021) 102091.

28 Pereira I, Monteiro C, Pereira-Silva M, Peixoto D, Nunes C, Reis S, Veiga F, Hamblin MR & Paiva-Santos AC, Nanodelivery systems for cutaneous melanoma treatment. *Eur J Pharm Biopharm*, 184 (2023) 214.

29 Asbaghi O, Ghanavati M, Ashtary-Larky D, Bagheri R, Rezaei Kelishadi M, Nazarian B, Nordvall M, Wong A, Dutheil F, Suzuki K & Alavi Naeini A, Effects of Folic Acid Supplementation on Oxidative Stress Markers: A Systematic Review and Meta-Analysis of Randomized Controlled Trials. *Antioxidants*, 10 (2021) 871.

30 Juzeniene A, Grigalavicius M, Ma LW & Juraleviciute M, Folic acid and its photoproducts, 6-formylpterin and pterin-6-carboxylic acid, as generators of reactive oxygen species in skin cells during UVA exposure. *J Photochem Photobiol B: Biol*, 155 (2016) 116.

31 Thomas AH, Lorente C, Capparelli AL, Martínez CG, Braun AM & Oliveros E, Singlet oxygen (1Δg) production by pterin derivatives in aqueous solutions. *Photochem Photobiol Sci*, 2 (2003) 245.

32 Yonny ME, Reineri PS, Palma GA & Nazareno MA, Development of an analytical method to determine malondialdehyde as an oxidative marker in cryopreserved bovine semen. *Anal Methods*, 7 (2015) 6331.

33 Aguilar Diaz De Leon J & Borges CR, Evaluation of Oxidative Stress in Biological Samples Using the Thiobarbituric Acid Reactive Substances Assay. *JoVE*, (2020) 61122.

34 Fogarasi E, Croitoru MD, Fülöp I, Nemes-Nagy E, Tripon RG, Simon-Szabo Z & Muntean DL, Malondialdehyde levels can be measured in serum and saliva by using a fast HPLC method with visible detection / Determinarea printr-o metodă HPLC-VIS rapidă a concentraţiilor serice şi salivare ale malondialdehidei. *Rev Rom Med Lab*, 24 (2016) 319.

35 Ansarin K, Khoubnasabjafari M & Jouyban A, Reliability of malondialdehyde as a biomarker of oxidative stress in psychological disorders. *Bioimpacts*, 5 (2017) 123.

36 Janero DR, Malondialdehyde and thiobarbituric acid-reactivity as diagnostic indices of lipid peroxidation and peroxidative tissue injury. *Free Radic Biol Med*, 9 (1990) 515.

37 Stasheuski AS, Galievsky VA, Knyukshto VN, Ghazaryan RK, Gyulkhandanyan AG, Gyulkhandanyan GV & Dzhagarov BM, Water-Soluble Pyridyl Porphyrins with Amphiphilic N-Substituents: Fluorescent Properties and Photosensitized Formation of Singlet Oxygen. *J Appl Spectrosc*, 80 (2014) 813.

38 Sun D, Zhang S, Wei Y & Yin L, Antioxidant activity of mangostin in cell-free system and its effect on K562 leukemia cell line in photodynamic therapy. *ABBS*, 41 (2009) 1033.

39 Saczko J, Kulbacka J, Chwiłkowska A, Lugowski M & Banaś T, Levels of lipid peroxidation in A549 cells after PDT *in vitro*. *Rocz Akad Med Bialymst*, 49 Suppl 1 (2004) 82.

40 Dennery PA, Vreman HJ, Rodgers PA & Stevenson DK, Role of Lipid Peroxidation in Metalloporphyrin-Mediated Phototoxic Reactions in Neonatal Rats. *Pediatr Res*, 33 (1993) 87.

41 Luiza Andreazza N, Vevert-Bizet C, Bourg-Heckly G, Sureau F, José Salvador M & Bonneau S, Berberine as a photosensitizing agent for antitumoral photodynamic therapy: Insights into its association to low density lipoproteins. *Int J Pharm*, 510 (2016) 240.

42 Wang S, Chen C, Wu J, Zhang J, Lam JWY, Wang H, Chen L & Tang BZ, A mitochondria-targeted AIE photosensitizer for enhancing specificity and efficacy of ferroptosis inducer. *Sci China Chem*, 65 (2022) 870.

43 Zhang Q i., Xiang G, Zhang Y, Yang K, Fan W o., Lin J, Zeng F & Wu J, Increase of doxorubicin sensitivity for folate receptor positive cells when given as the prodrug N-(phenylacetyl) doxorubicin in combination with folate-conjugated PGA. *J Pharm Sci*, 95 (2006) 2266.

44 Bae B chan & Na K, Self-quenching polysaccharide-based nanogels of pullulan/folate-photosensitizer conjugates for photodynamic therapy. *Biomaterials*, 31 (2010) 6325.

45 Henderson GB, Folate-Binding Proteins. *Annu Rev Nutr*, 10 (1990) 319.